

# Supplementary Materials for “Frustration shapes multi-channel Kondo physics: a star graph perspective”

Siddhartha Patra,<sup>1,\*</sup> Abhirup Mukherjee,<sup>1,†</sup> Anirban Mukherjee,<sup>1,‡</sup>

N. S. Vidhyadhiraja,<sup>2,§</sup> A. Taraphder,<sup>3,¶</sup> and Siddhartha Lal<sup>1,\*\*</sup>

<sup>1</sup>*Department of Physical Sciences, Indian Institute of Science Education and Research-Kolkata, W.B. 741246, India*

<sup>2</sup>*Theoretical Sciences Unit, Jawaharlal Nehru Center for Advanced Scientific Research, Jakkur, Bengaluru 560064, India*

<sup>3</sup>*Department of Physics, Indian Institute of Technology Kharagpur, Kharagpur 721302, India*

(Dated: June 30, 2022)

## I. ADDITIONAL PROPERTIES OF THE STAR GRAPH

### A. Energy lowering due to quantum fluctuations

The star graph Hamiltonian that sits at the heart of the RG fixed point Hamiltonian of the multichannel Kondo model contains a classical Ising term and a quantum fluctuation term:

$$H = \mathcal{J} \vec{S}_d \cdot \vec{S} = \mathcal{J} \left[ \underbrace{S_d^z S^z}_{\text{Ising term}} + \underbrace{\frac{1}{2} (S_d^+ S^- + \text{h.c.})}_{\text{quantum fluctuation part}} \right] = \mathcal{J} [\mathcal{H}^C + \mathcal{H}^Q] . \quad (1)$$

We are interested in studying how the presence of quantum fluctuations in the Hamiltonian of eq. 1 stabilises the ground state. This can be understood by looking at the contributions, per channel, of the classical and the quantum parts to the total ground state energy  $E_g$ . In the over-screened case ( $K > 2S_d$ ), the contributions are

$$E_C = \frac{1}{K} \langle \psi_g | \mathcal{H}^C | \psi_g \rangle, \quad E_Q = \frac{1}{K} \langle \psi_g | \mathcal{H}^Q | \psi_g \rangle = \frac{E_g/\mathcal{J} - E_C}{K} = -\frac{1}{2} S_d - \frac{1}{K} (S_d + E_C) , \quad (2)$$

where we have defined the contributions  $E_C$  and  $E_Q$  to the ground state energy coming from the Ising and fluctuation parts respectively, and we have substituted the ground state energy  $E_g$  for the over-screened case from eq.(10) in the main text. This contribution  $E_Q$  is generated by the spin-flip fluctuations between the impurity spin and the outer spins of the star graph. Note that because of the degeneracy of the ground state subspace, there are multiple ground states characterised by different values of  $J^z = S^z + S_d^z$ , and different ground states lead to different values of  $E_Q$ .

The variation of  $E_Q$  is shown in Fig.1 for the case of  $S_d = 1/2$ , as functions of the number of channels  $K$  as well as the ground state value  $J^z$  in which  $E_Q$  is being calculated. For a particular channel  $K$ , we find that the maximum  $|E_Q|$  is obtained for the state with smallest magnitude of  $J^z$  ( $J^z = 0$  for odd  $K$  and  $J^z = \pm 1/2$  for even  $K$ ), whereas  $|E_Q|$  is minimum in the states with largest  $J^z$  ( $J^z = \pm J$ ). The larger values of  $|E_Q|$  indicate that the quantum fluctuations are largest in the states with minimum  $J^z$ , and these states can be thought of as the counterparts to the maximally entangled singlet seen in the single-channel Kondo problem. This behaviour persists as  $K \gg 1$ : the magnitude  $|E_Q|$  associated with the  $|J^z| = J$  states vanish, showing the classical nature of these states and the lack of quantum fluctuations in that limit. On the other hand, the state  $|J^z| = |J^z|_{\min}$  has a non-zero  $|E_Q|$  in the large  $K$  limit and hence contains some non-zero quantum fluctuations, showing the true quantum nature of this macroscopic singlet state.

### B. Measure of quantum fluctuations

Here we are interested in calculating the quantum fluctuation present in the ground state by measuring the expectation value of the spin-flip part of the Hamiltonian:  $\mathcal{Q} \equiv \langle \psi_g | (J^x)^2 + (J^y)^2 | \psi_g \rangle = \langle \psi_g | J^2 - (J^z)^2 | \psi_g \rangle$ . For

\* sp14ip022@iiserkol.ac.in

† am18ip014@iiserkol.ac.in

‡ mukherjee.anirban.anirban@gmail.com

§ raja@jncasr.ac.in

¶ arghya@phy.iitkgp.ernet.in

\*\* slal@iiserkol.ac.in

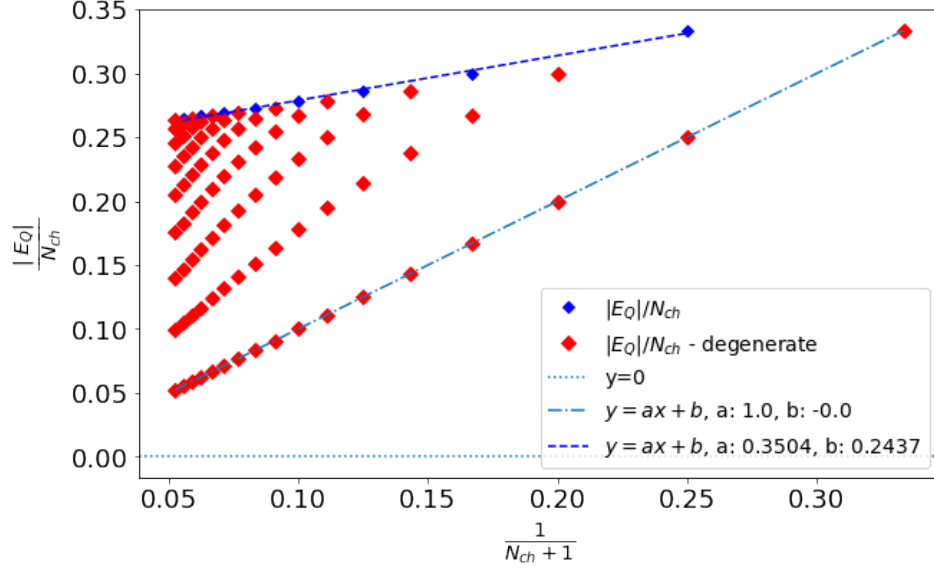


FIG. 1. This shows the variation of quantum energy per channel with  $1/N$ , where  $N = N_{ch} + 1$  is the total number of spins in the systems including the impurity spins.

a general spin- $S_d$  impurity, the ground state is characterised by  $J = |K/2 - S_d|$ , which gives  $J^2 = J(J + 1) = (|K/2 - S_d|)(|K/2 - S_d| + 1)$ . We define  $\Delta = (K/2 - S_d)$  to quantify the deviation from exact screening;  $\Delta = 0$  represents the exactly screened problem, and  $\Delta > 0$  and  $\Delta < 0$  represents the over-screened and under-screened problems respectively. Among the degenerate ground state, the maximum quantum fluctuation will occur in the state with minimum  $|J^z|$ . Since  $J$  can actually be written as  $J = |\Delta|$ ,  $J$  will take integer values when  $\Delta$  is integer, and the minimum value of  $|J^z|$  is then zero. Otherwise, when  $\Delta$  is half-integer,  $J$  will also take half-integer values, and the minimum value of  $|J^z|$  is  $1/2$ . With these considerations, the minimum value of the quantum fluctuation, *per channel*, is

$$q_K = \frac{1}{K} \sqrt{Q_{\max}} = \frac{1}{K} \sqrt{\langle \psi_g | J^2 - |J^z|_{\min}^2 | \psi_g \rangle} = \begin{cases} \frac{1}{K} \sqrt{(|K/2 - S_d|)(|K/2 - S_d| + 1) - 1/4}, & \text{where } \Delta \text{ is half-integer} \\ \frac{1}{K} \sqrt{(|K/2 - S_d|)(|K/2 - S_d| + 1)}, & \text{where } \Delta \text{ is integer} \end{cases} \quad (3)$$

This expression is symmetric under the transformation  $\Delta \rightarrow -\Delta$ , and represents a duality between the over-screened and under-screened models. In the limit of large channel number  $K$ ,  $q_K$  simplifies to  $\lim_{K \rightarrow \infty} q_K = \lim_{K \rightarrow \infty} \frac{1}{2K} |\Delta(K)|$ . Only the over- and under-screened models have non-vanishing (and equal) values of  $q_K$ .

### C. Staggered magnetization of the star graph

Another probe to study the screening as a function of  $K$  is the staggered magnetization  $\vec{M}_s = \vec{S} - \vec{S}_d$ . One can rewrite the Hamiltonian as  $\vec{S}_d \cdot \vec{S} = \frac{1}{4}[J^2 - M_s^2]$ . Since  $J$  and  $M_s$  commute with each other and hence also with the Hamiltonian, the eigenvalues of  $\vec{J}^2$  and  $M_s^2$  act as good quantum numbers for in the ground states of the star graph model. The larger the value of  $\langle M_s^2 \rangle$ , the stronger is the screening in that ground state. For single-channel case with  $K = 1$ , the ground state is a unique 2-spin singlet  $|\psi_g\rangle = \frac{1}{\sqrt{2}}(|\uparrow\downarrow\rangle - |\downarrow\uparrow\rangle) = |J = 0, J_z = 0\rangle$ , and the staggered magnetization per direction is  $M_s^2/3 = 1$ , which shows the perfect screening.

Calculating the staggered magnetization for a general multichannel problem with  $K$  channels and a spin- $S_d$  impurity reveals the breakdown of screening brought about by the presence of multiple channels. We find, in general, that the square of the staggered magnetization per channel is

$$m_s^2 = \left\langle \left( \frac{1}{K} M_s \right)^2 \right\rangle = \frac{1}{K^2} \langle \psi_g | (\vec{S}_d - \vec{S})^2 | \psi_g \rangle = \frac{1}{K^2} \langle \psi_g | 2(\vec{S}_d^2 + \vec{S}^2) - \vec{J}^2 | \psi_g \rangle = \frac{2S_d(S_d + 1)}{K^2} + \frac{1}{4} + \frac{1}{K} + \frac{1}{4K^2} \quad (4)$$

This shows that as the number of channels increases, the value of  $m_s^2$  decreases from the perfectly-screened value of 3. For  $K \rightarrow \infty$  and keeping  $S_d$  finite,  $m_s^2$  approaches a lowered value of  $1/4$ .

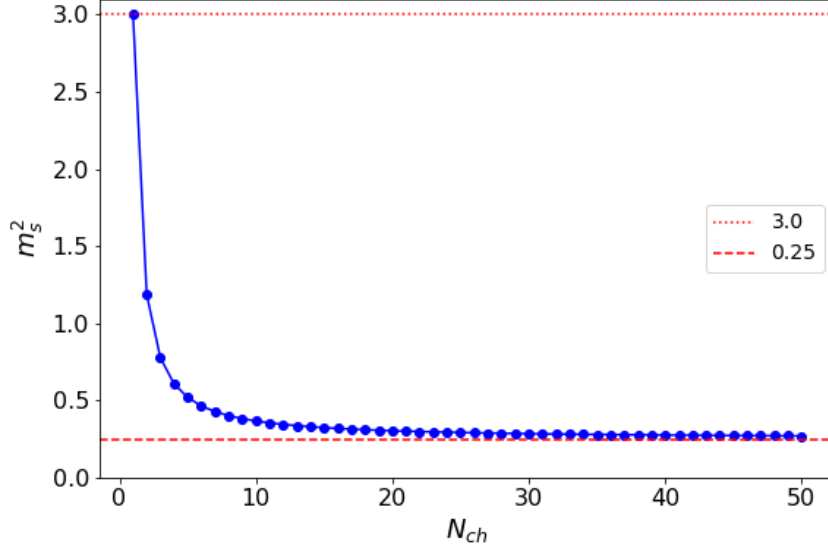


FIG. 2. This shows how the staggered magnetization changes with the number of channels  $N_{ch}$ .

Due to the  $SU(2)$  symmetry of the problem, the staggered magnetisation is the same along each of the three directions, such that the total value  $m_s^2$  is three times the value in any particular direction:

$$\langle (m_s^x)^2 \rangle = \langle (m_s^y)^2 \rangle = \langle (m_s^z)^2 \rangle = \frac{1}{3} m_s^2, \quad (5)$$

As mentioned above, the single channel case displays a value of  $\langle (m_s^z)^2 \rangle = 1$ , showing the perfect screening. If one takes the limit of  $K \rightarrow \infty$  keeping  $S_d = K/2$ , we get the staggered magnetisation at exact-screening and large  $K$ , and the value is  $\langle (m_s^z)^2 \rangle = 1/4$ . This is reduced from the value at  $K = 1$ . This reduced value however is still greater than the value of  $1/12$  reached as  $K \rightarrow \infty$  away from exact-screening by keeping  $S_d$  finite. These conclusions can be easily understood from fig.2 where we have shown the variation of  $\langle m_s^2 \rangle$  as a function of  $K$ , keeping  $S_d = 1/2$ .

#### D. Thermodynamic quantities

##### 1. Impurity magnetization in terms of parity operators

Just like the complete string operator  $\pi^z$ , the modified string operator  $\sigma_d^z \pi^z$  is also a Wilson loop operator that wraps around only the outer nodes of the star graph:

$$\pi_c^z \equiv \sigma_d^z \pi^z = \exp \left[ i \frac{\pi}{2} \left( \sum_{l=1}^K \sigma_l^z - K \right) \right]. \quad (6)$$

The expectation value of the impurity magnetization along a particular direction and in specific ground states can be related to the 't Hooft operator. We will work in the state comprised of two adjacent eigenstates of  $J^z$ :

$$|g_{J^z}^\theta\rangle \equiv \frac{1}{\sqrt{2}} (|J^z\rangle + e^{i\theta} |J^z + 1\rangle), \quad J^z < \frac{1}{2}(K-1). \quad (7)$$

The expectation value of the impurity magnetization operator  $\sigma_d^x$  can be expressed as

$$\langle \sigma_d^x \rangle \equiv \langle g_{J^z}^\theta | \sigma_d^x | g_{J^z}^\theta \rangle = -\langle J^z + 1 | \pi_c^x | J^z \rangle + \text{h.c.} \quad (8)$$

This expression relates the observable impurity magnetization to the topological 't Hooft operator [1]. Evaluating the matrix elements gives

$$\langle \sigma_d^x \rangle = -\frac{\sqrt{K^2 - (2J^z + 1)^2}}{2(1 + K)} \cos \theta. \quad (9)$$

Performing a similar calculation reveals that the impurity magnetizations along  $y$  and  $z$  in the same state are given by

$$\langle \sigma_d^y \rangle = -\frac{\sqrt{K^2 - (2J^z + 1)^2}}{2(1 + K)} \sin \theta, \quad \langle \sigma_d^z \rangle = -\frac{2J^z + 1}{(1 + K)}. \quad (10)$$

Combining eqs. 9 and 10, we find

$$\cos^2 \theta (\langle \sigma_d^x \rangle)^2 + \sin^2 \theta (\langle \sigma_d^y \rangle)^2 + \frac{1}{4} (\langle \sigma_d^z \rangle)^2 = \frac{1}{4} \left( \frac{K}{1 + K} \right)^2. \quad (11)$$

This relation *constrains the values of the magnetization* in all the directions: the  $x$  and  $y$  magnetization values have already been shown to be related to the 't Hooft operators  $\pi^x$  and  $\pi^y$  and the magnetization along  $z$  is therefore constrained in terms of the 't Hooft operators and the quantized function on the right-hand side (the function is quantized because  $K$  can only take integer values).

## 2. Thermal entropy

The star graph model can be solved to obtain the partition function, and this then allows the computation of the Helmholtz free energy and hence the thermal entropy:

$$\mathcal{F} = -k_B T \log Z, \quad S = -\frac{\partial \mathcal{F}}{\partial T} = -k_B \log Z - k_B T \frac{1}{Z} \frac{dZ}{dT} = -k_B \log \sum_{\epsilon} d(\epsilon) e^{-\beta \epsilon} - \frac{1}{\beta} \frac{k_B \sum_{\epsilon} \epsilon d(\epsilon) e^{-\beta \epsilon} \beta^2}{\sum_{\epsilon} d(\epsilon) e^{-\beta \epsilon}}, \quad (12)$$

where  $d(\epsilon)$  is the degeneracy of the state at energy  $\epsilon$ . The high and low-temperature limits take very simple forms:

$$\lim_{\beta \rightarrow \infty} S = -k_B \log_2 d(\epsilon_G), \quad \lim_{\beta \rightarrow 0} S = -k_B \log \sum_{\epsilon} d(\epsilon). \quad (13)$$

In fig.3, we plot the thermal entropy (in units of  $k_B \log 2$ ) for a range of temperatures and for different values of  $K$ . At large temperatures,  $S$  saturates to integer multiples of  $k_B \log 2$ , while at low-temperatures, that is not always the case. This is because the total Hilbert space dimension  $\sum_{\epsilon} d(\epsilon)$  is simply  $2^N$  ( $N$  being the total number of 1-particle states in the Hilbert space), and therefore  $\log \sum_{\epsilon} d(\epsilon) = N \log 2$  is always an integer multiple of  $N$ . On the other hand, the ground state degeneracy  $d(\epsilon_G)$  is  $|K - 2S_d|$  which is not necessarily of the form  $2^N$  and hence does not always lead to an integer multiple of  $\log 2$ .

## II. ADDITIONAL TOPOLOGICAL FEATURES OF THE LOCAL MOTT LIQUID

### A. Non-local twist operators and ground state degeneracy

The all-to-all Hamiltonian obtained by resolving the impurity-bath quantum fluctuations is written in terms of the spinor spin operators which are individually made out of two electronic degrees of freedom.

$$H_{eff} = \frac{\beta_{\uparrow}(\mathcal{J}, \omega_{\uparrow})}{4} (S^+ S^- + S^- S^+), \quad (14)$$

where  $\beta_{\uparrow}(\mathcal{J}, \omega_{\uparrow}) = (\mathcal{J}^2 \Gamma_{\uparrow})/2$ ,  $\Gamma_{\uparrow} = (\omega_{\uparrow} - \mathcal{J}(S_d^z - 1))^{-1}$ . This spin operator is defined as  $\vec{S}_i = \frac{\hbar}{2} \sum_{\alpha, \beta \in \{\uparrow, \downarrow\}} c_{0\alpha}^{(i)\dagger} \vec{\sigma}_{\alpha\beta} c_{0\beta}^{(i)}$ .

In the above eq.(14) we see the  $U(1)$  symmetry of the effective Hamiltonian. Using the spinor representation, we obtain the spin creation operation in terms of the electronic degree of freedom:

$$S_i^+ = \frac{\hbar}{2} \sum_{\alpha, \beta \in \{\uparrow, \downarrow\}} c_{0\alpha}^{(i)\dagger} \sigma_{\alpha\beta}^+ c_{0\beta}^{(i)} = \frac{\hbar}{2} c_{0\uparrow}^{(i)\dagger} c_{0\downarrow}^{(i)}, \quad S_i^z = \frac{\hbar}{2} \sum_{\alpha, \beta \in \{\uparrow, \downarrow\}} c_{0\alpha}^{(i)\dagger} \sigma_{\alpha\beta}^z c_{0\beta}^{(i)} = \frac{\hbar}{2} (c_{0\uparrow}^{(i)\dagger} c_{0\uparrow}^{(i)} - c_{0\downarrow}^{(i)\dagger} c_{0\downarrow}^{(i)}). \quad (15)$$

This spinor is simply the Anderson pseudo-spin formulation in the spin channel. The spin-creation operator ( $S_i^+$ ) involves the simultaneous creation of an electron-hole pair at the real space origin of the  $i^{th}$  conduction channel. The

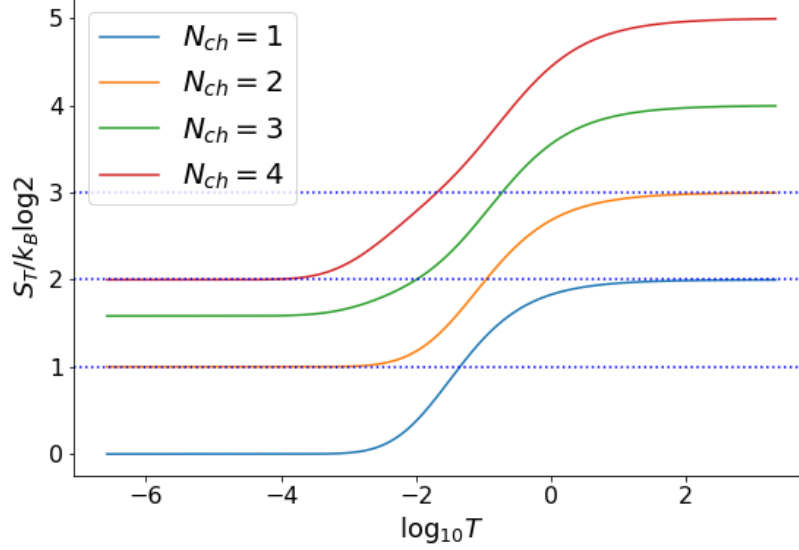


FIG. 3. This shows the variation of thermal entropy with the temperature.

condensation of such electron-hole pairs has already been shown in [2, 3]. Thus, for this effective Hamiltonian, one can define twist-translation operations to construct the gauge theory and unveil any hidden degeneracy.

Let's recall the effective Hamiltonian

$$H_{eff} = \frac{\beta_{\uparrow}(\alpha, \omega_{\uparrow})}{4} \left[ \sum_{ij} S_i^+ S_j^- + \text{h.c.} \right], \quad (16)$$

where  $i, j$  are the channel indices. Due to the all-to-all nature of the connectivity, one can draw a total of  $K!$  possible unique closed paths ( $\mathcal{C}_{\mu}$ ) such that each node (channel) is touched exactly once. These curves lead to  $K!$  translation operators ( $\hat{T}_{\mu}$ ) which keeps the Hamiltonian invariant. Let's define one such translation operator  $\hat{T}_{\mu} = e^{i\hat{P}_{\mu}^{cm}}$  which gives a periodic shift along the closed path  $\mathcal{C}_{\mu}$ . The twist operator along the path  $\mathcal{C}_{\mu}$  is given by

$$\hat{\mathcal{O}}_{\mu} = \exp\left(i \frac{2\pi}{K} \sum_{\substack{j=1 \\ \mathcal{C}_{\mu}}}^K j S_j^z\right), \quad (17)$$

The action of the translation operator on  $S_j^z$  is to translate it by one channel index:  $\hat{T}_{\mu} S_j^z \hat{T}_{\mu}^{\dagger} = S_{j+1}^z$  where  $j+1$  and  $j$  are the nearest neighbor on the closed path  $\mathcal{C}_{\mu}$ . Then the braiding rule between the twist and translation operators are give as

$$\hat{T}_{\mu} \hat{\mathcal{O}}_{\mu} \hat{T}_{\mu}^{\dagger} \hat{\mathcal{O}}_{\mu}^{\dagger} = \exp\left\{i\left[2\pi S_1^z - \frac{2\pi}{K} S^z\right]\right\} = \exp\left\{i\left[\pm\pi - \frac{2\pi}{K} S^z\right]\right\} = \exp\left(i \frac{2\pi p}{q}\right). \quad (18)$$

The availability of the non-trivial braiding statistics between these twist and translation operators is possible if  $p \neq 0$  and  $q \neq \infty$ . Further simplification leads to the condition

$$\pm\pi - \frac{2\pi}{K} S^z = \frac{2\pi p}{q} \implies \pm\frac{1}{2} - \frac{S^z}{K} = \frac{p}{q}, \quad \frac{(\pm K - 2S^z)}{2K} = \frac{p}{q}, \quad (19)$$

where  $p, q$  are mutual primes. We know that the  $S^z$  can take values  $(\mp K/2 \pm m)$  where  $m$  is a integer  $0 \leq m \leq K$ . Putting this value in the above equation leads to two possible solutions.

$$\frac{(K-m)}{K} = \frac{p}{q}, \quad \frac{-m}{K} = \frac{p}{q}. \quad (20)$$

For the first case where  $K - m = p$ , we can see that  $m = K$  makes  $p$  trivial, and hence the allowed values are  $m = 0, \dots, K - 1$ , which represents the corresponding  $S^z$  eigenvalues

$$-K/2, -K/2 + 1, \dots, K/2 - 2, K/2 - 1. \quad (21)$$

Similarly the second case implies,  $-m = p$ , but  $p = 0$  is not allowed as this makes the braiding statistics trivial, thus the possible  $S^z$  values are

$$-K/2 + 1, -K/2 + 2, \dots, K/2 - 1, K/2. \quad (22)$$

Thus we get the general braiding statistics between the twist and the translation

$$\hat{T}_\mu \hat{\mathcal{O}}_\mu \hat{T}_\mu^\dagger \hat{\mathcal{O}}_\mu^\dagger = e^{i \frac{2\pi p}{K}}, \quad (23)$$

where  $p$  corresponds to different  $S^z$  states, related as  $p = \pm K/2 - S^z$ . Thus we can see that there are  $K$  possible  $S^z$  plateau states in the all-to-all model where each plateau is  $K$  fold degenerate. This  $p/K$  is similar to the filling factor of the fractional quantum Hall effect. There are  $K!$  pairs of twist and translation operators corresponding to different closed paths  $\mathcal{C}_\mu$  which can probe this degeneracy.

### B. Action on the Hamiltonian

We will now obtain the action of these twist operators on the Hamiltonian in eq. 14. Due to the all-to-all nature of the effective Hamiltonian one can find  $K!$  possible relative arrangement of those  $K$  channels which keeps the Hamiltonian invariant. Here we briefly discuss the choice of the closed-loop  $\mathcal{C}_\mu$  and the insertion of the flux. As shown in the Fig.4(b) we have chosen a particular closed path which crosses all the outer spin only once. We embed that closed-loop on a plane and put the flux perpendicular to the plane through the closed loop. One can find a different closed loop where the ordering of the outer spins will be different. The action of the translation operator shifts the outer spins along this closed curve by one step.

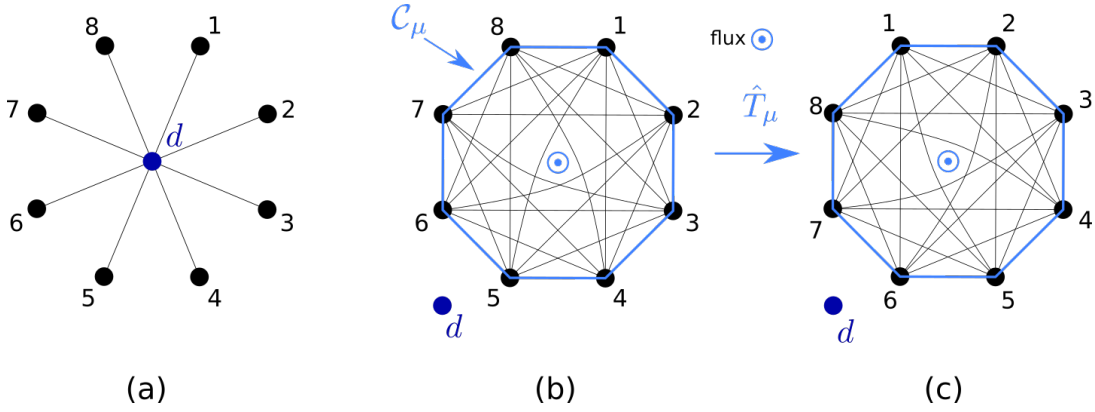


FIG. 4. (a) Schematic diagram of 8-channel multichannel Kondo model zero mode in zero bandwidth limit. (b) All-to-all model obtained by disentangling the impurity spin from the bath zero modes.  $\mathcal{C}_\mu$  is a particular closed curve. (c) Translated configuration along the curve  $\mathcal{C}_\mu$  by one unit.

The action of the twist operator on the  $S^x$  is determined in the following calculation

$$\hat{\mathcal{O}}_\mu S^x \hat{\mathcal{O}}_\mu^\dagger = \exp(i \frac{2\pi}{K} \sum_{j=1}^K j S_j^z) S^x \exp(-i \frac{2\pi}{K} \sum_{j=1}^K j S_j^z) = e^X S^x e^{-X}. \quad (24)$$

To simplify the calculation, we define  $i \frac{2\pi}{K} = \Omega$ , thus  $X = \Omega \sum_j j S_j^z$ . Thus we get

$$e^X S^x e^{-X} = S^x + [X, S^x] + \frac{1}{2!} [X, [X, S^x]] + \dots = \sum_l (S_l^x \cos \theta_l - S_l^y \sin \theta_l), \quad \theta_l = \frac{2\pi l}{K} e^X S^y e^{-X} = \sum_l (S_l^y \cos \theta_l + S_l^x \sin \theta_l). \quad (25)$$

As already defined,  $\theta_l = \frac{2\pi l}{K} = \frac{2\pi(K-n)}{K}$ , where  $n$  is an integer. We can see that in the large channel limit  $\theta_l$  becomes inter multiple of  $2\pi$ . Thus in the large channel limit

$$\lim_{K \rightarrow \infty} \hat{\mathcal{O}}_\mu H_{eff} \hat{\mathcal{O}}_\mu^\dagger = \frac{\beta_\uparrow(\alpha, \omega_\uparrow)}{2} \left[ \hat{\mathcal{O}}_\mu S^x \hat{\mathcal{O}}_\mu^\dagger \hat{\mathcal{O}}_\mu S^x \hat{\mathcal{O}}_\mu^\dagger + \hat{\mathcal{O}}_\mu S^y \hat{\mathcal{O}}_\mu^\dagger \hat{\mathcal{O}}_\mu S^y \hat{\mathcal{O}}_\mu^\dagger \right] = \frac{\beta_\uparrow(\alpha, \omega_\uparrow)}{2} \left[ S^{x2} + S^{y2} \right] = H_{eff},$$

$$\lim_{K \rightarrow \infty} [\hat{\mathcal{O}}, H_{eff}] = 0. \quad (26)$$

Since the translation operator  $\hat{T}_\mu = e^{i\hat{\mathcal{P}}_\mu}$  commutes with the Hamiltonian, so does the generator  $\hat{\mathcal{P}}_\mu$ . We can label the  $j^{th}$  state with the eigenvalues of this operator  $\hat{\mathcal{P}}_\mu$  as  $|p_\mu^j\rangle$ . The action of these twist and translation operators on these states are

$$\hat{T}_\mu |p_\mu^j\rangle = e^{i\hat{\mathcal{P}}_\mu} |p_\mu^j\rangle = e^{ip_\mu^j} |p_\mu^j\rangle, \quad \hat{T}_\mu \hat{\mathcal{O}}_\mu |p_\mu^j\rangle = \hat{\mathcal{O}}_\mu \hat{T}_\mu e^{i\frac{2\pi m}{K}} |p_\mu^j\rangle = \hat{\mathcal{O}}_\mu e^{i(\frac{2\pi m}{K} + p_\mu^j)} |p_\mu^j\rangle, \quad \frac{2\pi m}{K} \equiv p_\mu^m, \quad (27)$$

$$\hat{T}_\mu \left( \hat{\mathcal{O}}_\mu |p_\mu^j\rangle \right) = e^{i(p_\mu^m + p_\mu^j)} \left( \hat{\mathcal{O}}_\mu |p_\mu^j\rangle \right), \quad (28)$$

where  $m$  represents different  $S^z$  plateaux. This shows that  $\hat{\mathcal{O}}_\mu |p_\mu^j\rangle$  is again an eigenstate of the translation operator, but with an eigenvalue that is different from  $|p_\mu^j\rangle$ , and is thus orthogonal to  $|p_\mu^j\rangle$ . Similarly, one can in general show that  $\langle p_\mu^j | \hat{\mathcal{O}}_\mu^q | p_\mu^j \rangle = 0$ , where  $q$  is any integer. Also in the large  $K$  limit we can see from the eq.(26) that these different twisted states has same energy. Which shows that at each plateau state labeled by the  $S^z$  eigenvalue has  $K$  fold degenerate eigenstates labeled by the eigenvalue of the translation operators. The complete set of commuting observables is therefore formed by  $H, S^z, \hat{T}$ , and states can be labeled as  $|E, S_j^z, P_\mu^j\rangle$ .

### III. EFFECT OF CONDUCTION BATH EXCITATIONS ON THE FIXED POINT THEORY

#### A. Non-Fermi liquid signatures in momentum space for 2-channel Kondo

Obtaining the effective Hamiltonian involves obtaining the low energy excitations on top of the ground state of the star graph. The large-energy excitations involve spin flips. This guides the separation of the Hamiltonian into a diagonal and an off-diagonal piece:

$$H = H_d + V = \underbrace{H_0 + JS_d^z s_{\text{tot}}^z}_{H_d} + \underbrace{\frac{J}{2} S_d^+ s_{\text{tot}}^- + \text{h.c.}}_{V+V^\dagger} \quad (29)$$

We define  $V$  as the interaction term that decreases  $s_{\text{tot}}^z$  by 1:  $V |s_{\text{tot}}^z\rangle \rightarrow |s_{\text{tot}}^z - 1\rangle$ . Similarly, we define  $V^\dagger |s_{\text{tot}}^z\rangle \rightarrow |s_{\text{tot}}^z + 1\rangle$ . The Schrodinger equation for the ground state can be written as

$$E_{\text{gs}} |\Psi_{\text{gs}}\rangle = H |\Psi_{\text{gs}}\rangle = (H_d + V) |\Psi_{\text{gs}}\rangle \implies (E_{\text{gs}} - H_d) \sum C_{S_d^z, s_{\text{tot}}, s_{\text{tot}}^z} |S_d^z, s_{\text{tot}}, s_{\text{tot}}^z\rangle = V \sum C_{S_d^z, s_{\text{tot}}, s_{\text{tot}}^z} |S_d^z, s_{\text{tot}}, s_{\text{tot}}^z\rangle \quad (30)$$

$E_{\text{gs}}$  is the ground state energy, and can be replaced by the star graph ground state energy if we remove the kinetic energy cost via normal ordering:  $E_{\text{gs}} = -\frac{J}{2} \left( \frac{K}{2} + 1 \right)$ . Since the interaction part  $V$  only changes  $S_d^z \rightarrow -S_d^z$  and  $s_{\text{tot}}^z \rightarrow s_{\text{tot}}^z \pm 1$ , we can simplify the equation into individual smaller equations. For the state  $(s_{\text{tot}}, s_{\text{tot}}^z) = (1, 0)$ , equations are

$$E_{\text{gs}} \left| \frac{1}{2}, 1, 0 \right\rangle = \left( H_d + V \frac{1}{E_{\text{gs}} - H_d} V^\dagger \right) \left| \frac{1}{2}, 1, 0 \right\rangle, \quad E_{\text{gs}} \left| -\frac{1}{2}, 1, 0 \right\rangle = \left( H_d + V^\dagger \frac{1}{E_{\text{gs}} - H_d} V \right) \left| -\frac{1}{2}, 1, 0 \right\rangle. \quad (31)$$

These represent the Schrodinger equation for the states  $|S_d^z, 1, 0\rangle$ , and the right hand sides therefore give the effective Hamiltonians for those states. If we combine the states into a single subspace  $|1, 0\rangle = \left\{ \left| \frac{1}{2}, 1, 0 \right\rangle, \left| -\frac{1}{2}, 1, 0 \right\rangle \right\}$ , the effective Hamiltonian for this composite subspace becomes the sum of the two parts:

$$H_{\text{eff}}^{1,0} |1, 0\rangle \langle 1, 0| = (H_d + V G_0 V^\dagger + V^\dagger G_0 V) |1, 0\rangle, \quad (32)$$

where  $G_0 = (E_{\text{gs}} - H_d)^{-1}$ . To calculate these effective Hamiltonians, we will expand the denominator in powers of in  $H_0^n/J^{n+1}$ ,  $n = 0, 1, 2, \dots$ . Expanding up to  $n = 2$  and keeping at most two particle interaction terms, the effective Hamiltonian is

$$H_{\text{eff}}^{1,0} = H_0 + \frac{J^2}{2(E_{\text{gs}} + \frac{J}{2})} \left[ 1 + \frac{H_0 + (\frac{1}{2} + S_d^z) s_{\text{tot}}^+ X_{1,\text{tot}} - (\frac{1}{2} - S_d^z) s_{\text{tot}}^- X_{1,\text{tot}}^\dagger}{2(E_{\text{gs}} + \frac{J}{2})} + \frac{H_0^2}{(E_{\text{gs}} + \frac{J}{2})^2} - \frac{Z_{1,\text{tot}} H_0}{(E_{\text{gs}} + \frac{J}{2})^3} \right]. \quad (33)$$

We employed the definitions

$$X_{n,\text{tot}} \equiv \sum_l \sum_{k,k'} (\epsilon_k - \epsilon_{k'})^n c_{k\downarrow}^\dagger c_{k'\uparrow}, \quad Z_{1,\text{tot}} \equiv \sum_{k,k',l} (\epsilon_k - \epsilon_{k'}) \frac{1}{2} \left( c_{k\uparrow,l}^\dagger c_{k'\uparrow,l} - c_{k\downarrow,l}^\dagger c_{k'\downarrow,l} \right). \quad (34)$$

There are several non-Fermi liquid terms of the form  $s_{\text{tot}}^+ X_{1,\text{tot}}, s_{\text{tot}}^- X_{1,\text{tot}}^\dagger, Z_{1,\text{tot}} H_0$ . These arise because of the degenerate manifold and the increased availability of states in the Hilbert space for scattering, as compared to the unique singlet ground state of the single-channel Kondo model.

### B. Low-temperature thermodynamic behaviour

The non-Fermi liquid (NFL) nature of the effective Hamiltonian can be demonstrated through a calculation of certain thermodynamic quantities like the impurity specific heat and the magnetic susceptibility. We begin by calculating the self-energy of this NFL hamiltonian. In real space, one can extract a diagonal piece from the effective Hamiltonian by using the fermionic anticommutation relations.

$$H_{\text{eff}}^{\text{off},(2)}|_{\text{diag}} = -(16t^2/3)[(S_1^z)^2 + (S_2^z)^2], \quad (35)$$

the corresponding momentum space Hamiltonian is obtained from the Fourier transform:

$$H_{\text{eff}}^{\text{off},(2)}|_{\text{diag}} = -\frac{4t^2}{3} \frac{1}{N} \left[ \sum_{k,\sigma} n_{k\sigma} \left( 1 - \frac{1}{N} \sum_{k_2} n_{k_2,-\sigma} \right) + \sum_{k,\sigma} \tilde{n}_{k\sigma} \left( 1 - \frac{1}{N} \sum_{k_2} \tilde{n}_{k_2,-\sigma} \right) \right]. \quad (36)$$

The above relation leads to the self-energy correction to the kinetic energy, which is

$$\bar{\epsilon}_k - \epsilon_k = \Sigma_k = -\frac{4t^2}{3N^2} \left( 1 - \frac{N}{e^{(\epsilon_k - \mu)/k_B T} + 1} \right). \quad (37)$$

Using the self-energy we calculate the impurity specific heat defined as  $C_{\text{imp}} = C(J^*) - C(0)$  which is defined as

$$C_{\text{imp}} = \sum_{\Lambda,\sigma} \beta \left[ \frac{(\bar{\epsilon}_\Lambda)^2 e^{\beta \bar{\epsilon}_\Lambda}}{(e^{\beta \bar{\epsilon}_\Lambda} + 1)^2} - \frac{(\epsilon_\Lambda)^2 e^{\beta \epsilon_\Lambda}}{(e^{\beta \epsilon_\Lambda} + 1)^2} \right]. \quad (38)$$

Using the self-energy obtained above, we extract the low-temperature behaviour of the impurity specific heat in the two-channel model for  $t = 0.1$  and  $\mathcal{J} = 1$ , and it is shown in the left panel of fig. 5. We find that at low-temperatures, the Sommerfeld coefficient  $C_{\text{imp}}/T$  follows a logarithmic behaviour for the two-channel case, which is in agreement with the results known in the literature [4–25].

$$\frac{C_{\text{imp}}}{T} \propto \log T. \quad (39)$$

To calculate the magnetic susceptibility, we numerically diagonalise the low-energy effective Hamiltonian, and use the following expression:

$$\chi = \beta \left[ \frac{\sum e^{-\beta \bar{\epsilon}_\Lambda} \langle \tilde{S}^z 2 \rangle}{\sum e^{-\beta \bar{\epsilon}_\Lambda}} - \frac{\sum e^{-\beta \epsilon_\Lambda} \langle S^z 2 \rangle}{\sum e^{-\beta \epsilon_\Lambda}} \right]. \quad (40)$$

The result is shown in the right panel of fig. 5, and we find that at low temperatures, the susceptibility has a logarithmic behaviour.

$$\chi(T) \propto \log T \quad (41)$$

We also calculated the Wilson ratio  $C_{\text{imp}}/T\chi$ , and we find that taking up to three sites on each conduction channel leads to a value of  $W = 8.3$ , which is greater than the known value of  $8/3$  [4–25]. We find that taking less number of sites leads to a lower value of  $W$ , which shows that taking more number of sites will lead to a value of  $W$  that is lower than 8.3 and closer to  $8/3$ .



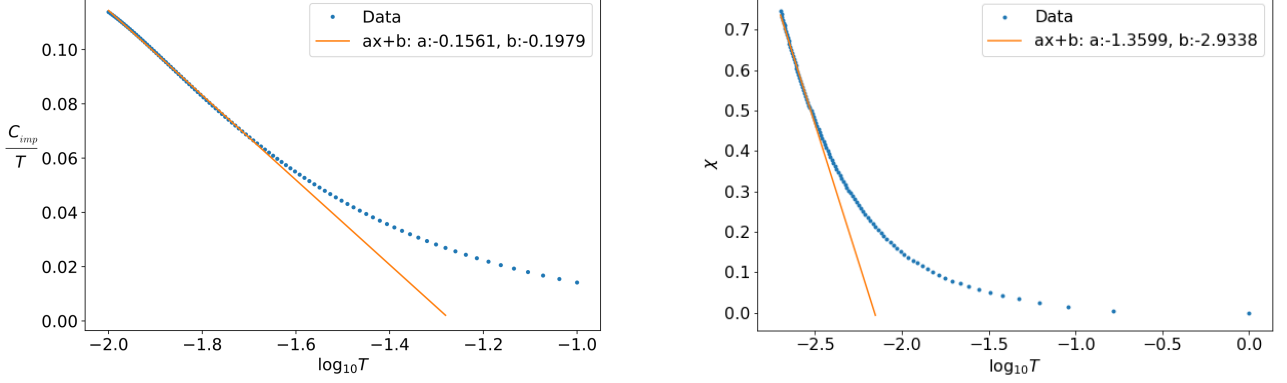


FIG. 5. Anomalous contribution to the impurity specific heat (left) and the magnetic susceptibility (right) arising from the non-Fermi liquid component

### C. Three channel LEH

Similar to the two channel case, we here calculate the low energy effective Hamiltonian for three channel Kondo problem by introducing the real space hopping on top of the zero mode three-channel star graph model. This zero mode three channel star graph model has three fold degenerate ground states with total  $2^4 = 16$  states in the eigenspectrum. The three degenerate ground states are given as

$$|\alpha_{-1}\rangle = c|1000\rangle - b(|0100\rangle + |0010\rangle + |0001\rangle), \quad |\alpha_{+1}\rangle = b(|1110\rangle + |1101\rangle + |1011\rangle) - c|0111\rangle, \quad (42)$$

$$|\alpha_0\rangle = -a(|1100\rangle + |1010\rangle + |1001\rangle) + a(|0110\rangle + |0101\rangle + |0011\rangle), \quad (43)$$

where  $a = 0.408$ ,  $b = 0.289$ ,  $c = 0.866$ . Here the state is represented by  $|n_d, n_1, n_2, n_3\rangle$ , where  $n_i = 1/0$  represents the spin configuration  $S_i^z = \pm 1/2$  respectively. Next we use degenerate perturbation theory to get the LEH which contains diagonal and off-diagonal terms. In this case we get non-zero contribution from all the three ground states  $|J^z = -1\rangle$ ,  $|J^z = 0\rangle$  and  $|J^z = 1\rangle$ . We get the diagonal contribution to the LEH in the second order to be

$$H_{eff,diag}^{(2)} = -\frac{7.2J^2}{\alpha} \hat{I}. \quad (44)$$

The contribution associated with different ground states  $|J^z = -1\rangle$ ,  $|J^z = 0\rangle$  and  $|J^z = 1\rangle$  is given respectively as  $-\frac{2.4J^2}{\alpha} \hat{I} + \hat{\mathcal{F}}$ ,  $-\frac{2.4J^2}{\alpha} \hat{I}$ ,  $-\frac{2.4J^2}{\alpha} \hat{I} - \hat{\mathcal{F}}$ , where  $\hat{\mathcal{F}}$  is a function of diagonal number operators of sites nearest neighbor to the zeroth site of each channels. The off-diagonal terms in the LEH is appearing due to the scattering between pair of degenerate states  $(\alpha_0, \alpha_{+1})$  and  $(\alpha_0, \alpha_{-1})$ , there is no contribution in the second order coming from the scattering between  $(\alpha_{-1}, \alpha_{+1})$ . The effective low energy Hamiltonian in the second order is given as

$$H_{eff,off-diag}^{(2)} = \sum_{\substack{(ijk)= \\ (123),(231),(312)}} \left[ c_{i\uparrow} c_{i\downarrow}^\dagger \left( -2ab \left\{ \Sigma_{jk} + c_{j\uparrow}^\dagger c_{j\downarrow} c_{k\uparrow} c_{k\downarrow}^\dagger \right\} - ac(\Omega_{jk} + \tilde{\Omega}_{jk}) \right) + \text{h.c.} \right] \otimes \hat{\Xi}_l, \quad (45)$$

where the different operators have the following definitions:

$$\Sigma_{i,j} = n_{i\uparrow}(1 - n_{i\downarrow})(1 - n_{j\uparrow})n_{j\downarrow} + (1 - n_{i\uparrow})n_{i\downarrow}n_{j\uparrow}(1 - n_{j\downarrow}), \quad \Omega_{i,j} = 4S_i^z S_j^z n_{i\uparrow} n_{j\uparrow}, \quad \tilde{\Omega}_{i,j} = 4S_i^z S_j^z (1 - n_{i\uparrow})(1 - n_{j\uparrow}), \quad (46)$$

$$\hat{\Xi}_l = (c_{l1\uparrow}^\dagger c_{l1\downarrow} + c_{l2\uparrow}^\dagger c_{l2\downarrow} + c_{l3\uparrow}^\dagger c_{l3\downarrow} + \text{h.c.}).$$

## IV. HAMILTONIAN RG OF SPIN-S IMPURITY MCK MODEL

### A. Details of the URG method

The non-trivial nature of the impurity problem arises from the fact that the many-particle correlation between the impurity spin and the conduction electrons induces a many-particle interaction among the conduction electron states.

This means that within the conduction band, the states at high and low energies get entangled with each other, leading to what is called UV-IR mixing. One of the methods of obtaining the low-energy physics while taking into account the effect of the high energy degrees of freedom is the renormalisation group (RG) approach. The specific variant of RG used in this work is the unitary renormalisation group (URG) method developed by some of us in Refs. [2, 3, 26–30]. The URG proceeds by applying unitary transformations on the Hamiltonian in order to decouple the high-energy  $k$ -states, leading to a reduction in the effective bandwidth and changes in the couplings for the low-energy degrees of freedom in the process. This leads to a sequence of renormalised Hamiltonians, and hence the coupling RG equations. While this is similar in spirit to the Poor Man's scaling approach of Anderson as applied to the single channel Kondo model [31], there are several differences between the methods that will be apparent when we describe the method in more detail below.

We start by defining a UV-IR scheme for the single-particle electronic states  $\vec{k} = (k_F + |\vec{k}|)\hat{k}$ . We label the single-particle  $\vec{k}$ -states in terms of their normal distance  $\Lambda = |\vec{k}|$  from the Fermi surface (FS) and the orientation of the unit vectors  $\hat{s} = \hat{k}$ , where  $\hat{s} = \frac{\nabla \epsilon_{\mathbf{k}}}{|\nabla \epsilon_{\mathbf{k}}|}|_{\epsilon_{\mathbf{k}}=E_F}$ . Each  $\hat{s}$  represents a direction that is normal to the FS. Combining these two labels with the spin index  $\sigma = \uparrow, \downarrow$ , each single-particle state can be uniquely labelled as  $|j, l\rangle = |(k_F + \Lambda_j)\hat{s}, \sigma\rangle$ ,  $l \equiv (\hat{s}, \sigma)$ . The  $\Lambda$ 's are arranged as follows:  $\Lambda_N > \Lambda_{N-1} > \dots > 0$ , such that  $\Lambda_N$  is farthest from the Fermi surface and is hence the most energetic (UV) while  $\Lambda_0$  is closest to the Fermi surface and is least energetic (IR). The URG proceeds by disentangling these states  $\Lambda_j$ , starting from those near the UV and gradually scaling towards the IR. This leads to the Hamiltonian flow equation [32]

$$H_{(j-1)} = U_{(j)} H_{(j)} U_{(j)}^\dagger, \quad (47)$$

where the unitary operation  $U_{(j)}$  is the unitary map at RG step  $j$ .  $U_{(j)}$  disentangles all the electronic states  $|\mathbf{k}_{\Lambda_j \hat{s}_m}, \sigma\rangle$  on the isogeometric curve and has the form [2, 32]

$$U_{(j)} = \prod_l U_{j,l}, U_{j,l} = \frac{1}{\sqrt{2}} \sum_l [1 + \eta_{j,l} - \eta_{j,l}^\dagger], \quad (48)$$

where  $l$  sums over the states on the isoenergetic shell at distance  $\Lambda_j$ , and  $\eta_{j,l}$  are electron-hole transition operators following the algebra

$$\{\eta_{j,l}, \eta_{j,l}^\dagger\} = 1, \quad [\eta_{j,l}, \eta_{j,l}^\dagger] = 2\hat{n}_{j,l} - 1. \quad (49)$$

The transition operator can be expressed in terms of the off-diagonal part of the Hamiltonian,  $H_{j,l}^X = Tr_{j,l}(c_{j,l}^\dagger H_j) c_{j,l} + \text{h.c.}$ , and the diagonal part  $H_{j,l}^D$  (kinetic energy and self-energies):

$$\eta_{j,l} = Tr_{j,l}(c_{j,l}^\dagger H_{j,l}) c_{j,l} \frac{1}{\hat{\omega}_{j,l} - Tr_{j,l}(H_{j,l}^D \hat{n}_{j,l}) \hat{n}_{j,l}}. \quad (50)$$

The off-diagonal operator  $Tr_{j,l}(c_{j,l}^\dagger H_{j,l}) c_{j,l}$  in the numerator of  $\eta_{j,l}$  contains all possible scattering vertices that change the configuration of the Fock state  $|j, l\rangle$  [32]. The generic forms of  $H_{j,l}^D$  and  $H_{j,l}^X$  are as follows

$$\begin{aligned} H_{j,l}^D &= \sum_{\Lambda \hat{s}, \sigma} \epsilon^{j,l} \hat{n}_{\mathbf{k}_{\Lambda \hat{s}}, \sigma} + \sum_{\alpha} \Gamma_{\alpha}^{4,(j,l)} \hat{n}_{\mathbf{k}\sigma} \hat{n}_{\mathbf{k}'\sigma'} + \sum_{\beta} \Gamma_{\beta}^{6,(j,l)} \hat{n}_{\mathbf{k}\sigma} \hat{n}_{\mathbf{k}'\sigma'} \hat{n}_{\mathbf{k}''\sigma''} + \dots, \\ H_{j,l}^X &= \sum_{\alpha} \Gamma_{\alpha}^2 c_{\mathbf{k}\sigma}^\dagger c_{\mathbf{k}'\sigma'} + \sum_{\beta} \Gamma_{\beta}^4 c_{\mathbf{k}\sigma}^\dagger c_{\mathbf{k}'\sigma'} c_{\mathbf{k}_1'\sigma_1'} c_{\mathbf{k}_1\sigma_1} + \dots \end{aligned} \quad (51)$$

The indices  $\alpha$  and  $\beta$  are strings that denote the quantum numbers of the incoming and outgoing electronic states at a particular interaction vertex  $\Gamma_{\alpha}^n$  or  $\Gamma_{\beta}^m$ . The operator  $\hat{\omega}_{j,l}$  accounts for the quantum fluctuations arising from the non-commutation between different parts of the renormalised Hamiltonian and has the following form [32]

$$\hat{\omega}_{j,l} = H_{j,l}^D + H_{j,l}^X - H_{j,l-1}^X. \quad (52)$$

Upon disentangling electronic states  $\hat{s}, \sigma$  along a isogeometric curve at distance  $\Lambda_j$ , the following effective Hamiltonian  $H_{j,l}$  is generated

$$H_{j,l} = \prod_{m=1}^l U_{j,m} H_{(j)} \left[ \prod_{m=1}^l U_{j,m} \right]^\dagger. \quad (53)$$

Accounting for only the leading tangential scattering processes, as well as other momentum transfer processes along the normal direction  $\hat{s}$ , the renormalised Hamiltonian  $H_{(j-1)}$  has the form [32]

$$Tr_{j,(1,\dots,2n_j)}(H_{(j)}) + \sum_{l=1}^{2n_j} \{c_{j,l}^\dagger Tr_{j,l}(H_{(j)} c_{j,l}), \eta_{j,l}\} \tau_{j,l} . \quad (54)$$

The RG fixed point is reached when the denominator in Eq. 50 vanishes, at a certain energy scale  $\Lambda^*$ . The vanishing of the denominator can be shown to be concomitant with the vanishing of the off-diagonal component  $H^X$  [32], and the fixed point value of the quantum fluctuation operator is equal to one of the eigenvalues of the Hamiltonian. The fixed point Hamiltonian  $H^*$  consists of the renormalised, still-entangled degrees of freedom  $\Lambda_j$  that lie inside the window  $\Lambda^*$ :  $\Lambda_j < \Lambda^*$ , as well as the integrals of motion (IOMs) that were decoupled by the URG transformations along the way. The IOMs have been stripped of any number fluctuations and are therefore diagonal in the basis of the number operators for each of the decoupled degrees of freedom.

$$H^* = \sum_{\Lambda_j < \Lambda^*} H^*(\Lambda_j) + \sum_{\Lambda_j > \Lambda^*} H_{\text{IOMs}}(\Lambda_j) \quad (55)$$

The effective Hamiltonian can be used to construct the corresponding thermal density matrix and hence the partition function at a temperature  $T$ :

$$Z^* = \text{Tr}[\rho^*] = \text{Tr}[e^{-\beta \hat{H}^*}] = \text{Tr}[U^\dagger e^{-\beta \hat{H}^*} U] = \text{Tr}[e^{-\beta \hat{H}}] = Z , \quad (56)$$

where  $\beta = 1/k_B T$ ,  $U = \prod_1^{j^*} U_{(j)}$ ,  $H$  is the bare Hamiltonian and  $j^*$  is the RG step at which the IR stable fixed point is reached. The unitary transformations preserve the partition function along the RG flow.

## B. Derivation of RG equation for the MCK model

The Hamiltonian for the channel-isotropic MCK model is:

$$H = \sum_l \left[ \sum_{\substack{k \\ \alpha=\uparrow,\downarrow}} \epsilon_{k,l} \hat{n}_{k\alpha,l} + \frac{\mathcal{J}}{2} \sum_{\substack{k,k' \\ \alpha,\alpha'=\uparrow,\downarrow}} \vec{S}_d \cdot \vec{\sigma}_{\alpha\alpha'} c_{k\alpha,l}^\dagger c_{k'\alpha',l} \right] . \quad (57)$$

The URG equation for the single-channel Kondo model [30] shows a stable strong coupling fixed point. Ferromagnetic interactions are irrelevant. Strictly speaking, that RG equation already encodes, in principle, the multi-channel behaviour, through a modified  $\hat{\omega}$ . To extract this information, we consider the strong coupling fixed-point  $J \gg D$  as a fixed point and analyze its stability from the star graph perspective. For the exactly-screened case, the star graph decouples from the conduction bath, leaving behind a local Fermi liquid interaction on the first site. Similarly, in the under-screened regime, the ground state is composed of states where the impurity spin is only partially screened by the conduction channels. If a particular configuration of the bath-impurity system has the total conduction bath spin down, the impurity will have a residual up spin. This induces a ferromagnetic super-exchange coupling that is irrelevant under RG, so this fixed point is stable as well.

We now come to the over-screened case, where there is a residual spin on the conduction channel site. The neighbouring electrons will now hop in with spins opposite to that of the impurity, so an antiferromagnetic interaction will be induced, and such an interaction is relevant under the RG. This shows that the over-screened regime cannot have a stable strong coupling fixed point, and we need to search for an intermediate coupling fixed point. We therefore need the generator of the unitary transformation that incorporates third order scattering scatterings explicitly. We should take account of all possible processes that render the set of states  $\{|\hat{n}_{q\beta} = 1\rangle, |\hat{n}_{q\beta} = 0\rangle\}$  diagonal. The higher order generator itself has two scattering processes, such that the entire renormalisation term  $c_{q\beta}^\dagger T \eta$  has in total three coherent processes. The complete generator up to third order can be written as

$$\eta = \frac{1}{\hat{\omega} - H_D} T^\dagger c \simeq \frac{1}{\omega' - H_D} T^\dagger c + \frac{1}{\omega' - H_D} H_X \frac{1}{\omega' - H_D} T^\dagger c + \frac{1}{\omega' - H_D} T^\dagger c \frac{1}{\omega' - H_D} H_X , \quad (58)$$

where  $H_X = J \sum_{k,k' < \Lambda_j, \alpha, \alpha'} \vec{S}_d \cdot \vec{\sigma}_{\alpha\alpha'} c_{k\alpha}^\dagger c_{k'\alpha'}$  is scattering between the entangled electrons. There are two third order terms in the above equation corresponding to the two possible sequences in which the processes can occur while

keeping the total renormalisation  $c_{q\beta}^\dagger T \eta$  diagonal in  $q\beta$ . The second order processes remain unchanged. The total renormalisation takes the form:

$$\Delta H_{(j)} = \underbrace{c^\dagger T \frac{1}{\omega' - H_D} T^\dagger c + (c^\dagger \leftrightarrow c)}_{\Delta H_{(j)}^{(2)}} + \underbrace{c^\dagger T \frac{1}{\omega' - H_D} H_X \frac{1}{\omega' - H_D} T^\dagger c + c^\dagger T \frac{1}{\omega' - H_D} T^\dagger c \frac{1}{\omega' - H_D} H_X + (c^\dagger \leftrightarrow c)}_{\Delta H_{(j)}^{(3)}} . \quad (59)$$

$\Delta H_{(j)}^{(2)}$  and  $\Delta H_{(j)}^{(3)}$  are the renormalisation arising from the second and third order processes respectively.

It is easier to see the RG flow of the couplings if we write the Hamiltonian in terms of the eigenstates of  $S_d^z$ . These eigenstates are defined by  $S_d^z |m_d\rangle = m_d |m_d\rangle$ ,  $m_d \in [-S, S]$ . In terms of these eigenstates, the Hamiltonian becomes

$$\mathcal{H} = \sum_{k\sigma} \epsilon_k \tau_{k\sigma} + \sum_{m_d=-S}^S \sum_{\substack{kl, \\ \sigma=\uparrow, \downarrow}} J_{m_d}^\sigma |m_d\rangle \langle m_d| c_{k\sigma}^\dagger c_{l\sigma} + \sum_{kl} \sum_{m_d=-S}^{S-1} J_{m_d}^t (|m_d+1\rangle \langle m_d| s_{kl}^- + \text{h.c.}) , \quad (60)$$

where  $k, l$  sum over the momentum states,  $\sigma$  sums over the spin indices,  $J_m^\sigma = \frac{1}{2} \sigma m J$  in the UV Hamiltonian, and  $J_m^t = J \frac{1}{2} \sqrt{S(S+1) - m(m+1)}$  is the coupling that connects  $|m\rangle$  and  $|m+1\rangle$ . We first calculate  $\Delta H_{(j)}^{(2)}$ . There will be two types of processes - those processes that start from an occupied state (particle sector) and those that start from a vacant state (hole sector). Due to particle hole symmetry of the Hamiltonian, they will be equal to each other and we will only calculate the particle sector contribution.

In the particle sector, we have ( $\hat{n}_{q\beta} = 1$ ), so we will work at a negative energy shell  $\epsilon_q = -D$ . The renormalisation can schematically be represented as  $H_0^I \frac{1}{\omega - H_{q\beta}^D} H_1^I$ . Both  $H_0^I$  and  $H_1^I$  have all three operators  $S_d^z, S_d^\pm$ . We first consider specifically the case of spin- $\frac{1}{2}$  impurity. Those terms that have identical operators on both sides can be ignored because  $S_d^{z2} = \text{constant}$  and  $S^{\pm 2} = 0$ . All the six terms that *will* renormalise the Hamiltonian have a spin flip operator on at least one side of the Greens function. This means that in the denominator of the Greens function,  $S_d^z$  and  $s_{qq}^z$  have to be anti-parallel in order to produce a non-zero result for that term. This means we can identically replace  $S_d^z s_{qq}^z = -\frac{1}{4}$ . Also, in the particle sector, the Greens function always has  $c_{q\beta}$  in front of it, so  $\epsilon_q \tau_{q\beta} = \frac{D}{2}$ . The upshot of all this is that the denominator of all scattering processes for the spin- $\frac{1}{2}$  impurity Hamiltonian will be  $\omega - \frac{D}{2} + \frac{J}{4}$ .

We now come to the general case of spin- $S$  impurity. The various terms that renormalise the Hamiltonian can be described in terms of the bath spin operators that come into them. For example, the term that has  $s^z$  on both sides of the intervening Greens function can be represented as  $z|z$ . There are 7 such terms:  $z|z, \pm|\mp, z|\pm, \pm|z$ . Each of these terms occurs both in the particle and the hole sectors. We will demonstrate the calculation of two of these terms. The  $z|z$  and  $|\pm$  terms evaluate in the following manner.

$$z|z : \sum_{kk', m, \sigma} c_{q\sigma}^\dagger c_{k'\sigma} |m\rangle \langle m| \frac{J_m^{\sigma 2}}{\omega - \frac{D}{2} + \frac{J}{2} \sigma S_d^z} |m\rangle \langle m| c_{k\sigma}^\dagger c_{q\sigma} = - \sum_{kk', m, \sigma} n_{q\sigma} \frac{J_m^{\sigma 2} c_{k\sigma}^\dagger c_{k'\sigma} |m\rangle \langle m|}{\omega_{m, \sigma} - \frac{D}{2} + \frac{J}{2} \sigma m} , \quad (61)$$

$$|\pm : \sum_{kk', m} c_{q\uparrow}^\dagger c_{k'\downarrow} |m\rangle \langle m+1| \frac{J_m^t 2}{\omega - \frac{D}{2} + \frac{J}{2} S_d^z} |m+1\rangle \langle m| c_{k\downarrow}^\dagger c_{q\uparrow} = -n_{q\uparrow} \sum_{kk', m} \frac{J_m^t 2 c_{k\downarrow}^\dagger c_{k'\downarrow} |m\rangle \langle m|}{\omega_{m+1, \uparrow} - \frac{D}{2} + \frac{J}{2} (m+1)} . \quad (62)$$

We similarly compute the rest of the terms. We again define  $\sum_q \hat{n}_{q\sigma} = n(D)$ . To compare with the spin- $\frac{1}{2}$  RG equations, we will transform the general spin- $S$   $\omega$  to the spin- $\frac{1}{2}$   $\omega$ , using  $\omega_{m, \sigma} \rightarrow \omega - \frac{J}{2} (m\sigma - \frac{1}{2})$ . The renormalisation in  $J_m^\sigma$  is

$$\Delta J_m^\sigma = -n(D) \frac{(J_m^\sigma)^2 + \left(J_{m-\frac{1+\sigma}{2}}^t\right)^2}{\omega - \frac{D}{2} + \frac{J}{4}} . \quad (63)$$

Here, we have defined  $J_m^t = 0$  for  $|m| > S$ . Two relations can be obtained from this RG equation, the RG equations for the sum and difference of the couplings:  $J_m^\pm = \frac{1}{2} (J_m^\uparrow \pm J_m^\downarrow)$ . The RG equation for the sum of the couplings is

$$\Delta J_m^+ = -n(D) \frac{\sum_\sigma (J_m^\sigma)^2 + \sum_\sigma \left(J_{m-\frac{1+\sigma}{2}}^t\right)^2}{2 \left(\omega - \frac{D}{2} + \frac{J}{4}\right)} = -n(D) \frac{J^2}{4} \frac{S(S+1)}{\omega - \frac{D}{2} + \frac{J}{4}} . \quad (64)$$

This is an  $m$ -independent piece, so it can be summed over to produce an impurity-independent potential scattering term, which we ignore.

The second is the RG equation for the difference of the couplings:

$$\Delta J_m^- = -n(D) \frac{1}{2} \frac{(J_{m-1}^t)^2 - (J_m^t)^2}{\omega - \frac{D}{2} + \frac{J}{4}} = -\frac{1}{4} \frac{n(D)mJ^2}{\omega - \frac{D}{2} + \frac{J}{4}}. \quad (65)$$

The usual  $J$  Kondo coupling is recovered through  $J = 2J_m^-/m$ . Substituting this gives

$$\Delta_{\text{p sector}} J = -\frac{1}{2} n(D) \frac{J^2}{\omega - \frac{D}{2} + \frac{J}{4}}. \quad (66)$$

We can also obtain the RG equation for  $J$  from the transverse renormalisation:

$$\Delta J_m^t = -\frac{n(D)J_m^t (J_m^\downarrow + J_{m+1}^\uparrow)}{\omega - \frac{D}{2} + \frac{J}{4}} = -\frac{1}{2} \frac{n(D)J_m^t J}{\omega - \frac{D}{2} + \frac{J}{4}}. \quad (67)$$

Since  $J_m^t \propto J$ , we have

$$\Delta J_{\text{p sector}} = -\frac{1}{2} \frac{n(D)J^2}{\omega - \frac{D}{2} + \frac{J}{4}}. \quad (68)$$

The total renormalisation from both particle and hole sectors, at this order, is

$$\Delta J^{(2)} = -\frac{n(D)J^2}{\omega - \frac{D}{2} + \frac{J}{4}}. \quad (69)$$

We now come to the third-order renormalisation. Following eq. 59, the next order renormalisation is

$$\Delta H_j^{(3)} = c^\dagger T \frac{1}{\omega' - H_D} H_X \frac{1}{\omega' - H_D} T^\dagger c + c^\dagger T \frac{1}{\omega' - H_D} T^\dagger c \frac{1}{\omega' - H_D} H_X. \quad (70)$$

The first term will be of the form

$$\sum_{q,k,l_1} c_{q\beta,l_1}^\dagger c_{k\alpha,l_1} |m_1\rangle \langle m_2| \frac{1}{\omega - \frac{D}{2} - \frac{\epsilon_k}{2} + \frac{\beta J}{4} S_d^z} |m_2\rangle c_{k_1\sigma_1,l_2}^\dagger c_{k_2\sigma_2,l_2} \langle m_3| \frac{1}{\omega - \frac{D}{2} - \frac{\epsilon_k}{2} + \frac{\beta J}{4} S_d^z} |m_3\rangle \langle m_4| c_{k\alpha,l_1}^\dagger c_{q\beta,l_1}. \quad (71)$$

We have not bothered to write all the summations and the couplings correctly, because we will only simplify the denominator here. Evaluating the inner products gives

$$\sum_{q,k,l_1} \frac{|m_1\rangle \langle m_4| c_{q\beta}^\dagger c_{k\alpha} c_{k_1\sigma_1,l_2}^\dagger}{\omega_{m_2,\beta} - \frac{D}{2} - \frac{\epsilon_k}{2} + \frac{\beta J m_2}{4}} \frac{c_{k_2\sigma_2,l_2} c_{k\alpha}^\dagger c_{q\beta}}{\omega_{m_3,\beta} - \frac{D}{2} - \frac{\epsilon_k}{2} + \frac{\beta J m_3}{4}}. \quad (72)$$

We again use  $\omega_{m,\sigma} \rightarrow \omega - \frac{J}{2} (m\sigma - \frac{1}{2})$ .

$$|m_1\rangle \langle m_4| c_{k_1\sigma_1,l_2}^\dagger c_{k_2\sigma_2,l_2} \sum_{q,k,l_1} \frac{\hat{n}_{q\beta} (1 - \hat{n}_{k\alpha})}{(\omega - \frac{D}{2} - \frac{\epsilon_k}{2} + \frac{J}{4})^2}. \quad (73)$$

We define  $\sum_q \hat{n}_{q\beta} = n(D)$ . Performing the sums over  $k$  and  $l_1$  gives

$$-\frac{1}{2} |m_1\rangle \langle m_4| c_{k_1\sigma_1,l_2}^\dagger c_{k_2\sigma_2,l_2} \frac{\rho n(D)K}{\omega - \frac{D}{2} + \frac{J}{4}}. \quad (74)$$

$\rho$  is the density of states which we have taken to be constant. Reinstating the complete summation and the couplings gives

$$-\frac{1}{2} \frac{\rho n(D)K}{\omega - \frac{D}{2} + \frac{J}{4}} \sum_{\substack{m_1, m_4, k_1, k_2, \\ l_2, \sigma_1 \sigma_2}} \lambda_1 \lambda_2 \lambda_3 |m_1\rangle \langle m_4| c_{k_1\sigma_1,l_2}^\dagger c_{k_2\sigma_2,l_2}. \quad (75)$$

There is no sum over  $m_2$  and  $m_3$  because they are constrained by  $m_1$  and  $m_4$  respectively.  $\lambda_i$  represent the couplings present at the three interaction vertices.  $k_{1,2}$  sum over the momenta,  $\sigma_{1,2}$  sum over the spin indices and  $l_2$  sums over the channels.

The second term in eq. 70 can be evaluated in an almost identical fashion. The integral here will be negative of the first term, because of an exchange in the scattering processes.

$$\frac{1}{2} \frac{\rho n(D)K}{\omega - \frac{D}{2} + \frac{J}{4}} \sum_{\substack{m_1, m_4, k_1, k_2, \\ l_2, \sigma_1 \sigma_2}} \lambda_1 \lambda_3 \lambda_2 |m_1\rangle \langle m_4| c_{k_1 \sigma_1, l_2}^\dagger c_{k_2 \sigma_2, l_2} . \quad (76)$$

The first group of terms (those that appear in 75) in the particle sector can be represented as  $a|b\rangle|c$ , where  $a, b, c \in \{z, +, -\}$  and represent the operator for the conduction electrons in the three connected processes. The  $l$  on  $b$  indicates that it is the state of the electrons *not being decoupled*. The second group of terms (those that appear in 76) are therefore represented as  $a|b\rangle|c'$ , because in this group, the interaction  $H_X$  between the electrons that are not being decoupled occur at the very end. We will only calculate the terms in the particle sector, the ones in hole sector will be equal to these because of particle-hole symmetry. The full list of terms is:

$$\begin{array}{cccccccccccccccc} z|z'|z & z|z|z' & -|z'|+ & -|+|z' & +|z'|z & +|z'|z & z|+|z & z|-|z & +|+|z & -|+|z & z|z|+ & z|z|- & +|-|+ & +|-|z' & -|+|+ & z|z|z & z|z|z' & -|z'|+ & -|+|z' & +|z'|z & +|z'|z & z|+|z & z|-|z & +|+|z & -|+|z' & -|+|+ & z|z|+ & z|z|- & +|-|+ & +|-|z' & -|+|+ & z|z|z & z|z|z' & -|z'|+ & -|+|z' & +|z'|z & +|z'|z & z|+|z & z|-|z & +|+|z & -|+|z' & -|+|+ \end{array}$$

The total renormalisation in  $J_m^\sigma$  is

$$\Delta J_m^\sigma = \frac{1}{2} \frac{\rho n(D)K}{\omega - \frac{D}{2} + \frac{J}{4}} \left[ (J_{m-1}^t)^2 J_m^\sigma + (J_m^t)^2 J_m^\sigma - (J_{m-1}^t)^2 J_{m-1}^\sigma - (J_m^t)^2 J_{m+1}^\sigma \right] = \frac{1}{2} \frac{\rho n(D)K}{\omega - \frac{D}{2} + \frac{J}{4}} J^3 m \sigma . \quad (77)$$

Since we had defined  $J_m^\sigma \equiv \frac{1}{2} J m \sigma$ , we have  $\Delta J = \frac{2}{m \sigma} \Delta J_m^\sigma$ , and we get  $\Delta_{\text{p sector}} J = \frac{1}{4} \frac{\rho n(D)K}{\omega - \frac{D}{2} + \frac{J}{4}} J^3$ . Combining with the hole sector renormalisation, we get

$$\Delta J^{(3)} = \frac{1}{2} \frac{\rho n(D)K}{\omega - \frac{D}{2} + \frac{J}{4}} J^3 . \quad (78)$$

The total renormalisation in  $J$  after combining all orders is

$$\Delta J = -\frac{n(D)J^2}{\omega - \frac{D}{2} + \frac{J}{4}} + \frac{1}{2} \frac{\rho n(D)K}{\omega - \frac{D}{2} + \frac{J}{4}} J^3 . \quad (79)$$

- 
- [1] V. Marić, S. M. Giampaolo, and F. Franchini, Communications Physics **3**, 220 (2020).
  - [2] A. Mukherjee and S. Lal, New Journal of Physics **22**, 063007 (2020).
  - [3] A. Mukherjee and S. Lal, New Journal of Physics **22**, 063008 (2020).
  - [4] I. Affleck and A. W. Ludwig, Nuclear Physics B **360**, 641 (1991).
  - [5] A. W. W. Ludwig and I. Affleck, Phys. Rev. Lett. **67**, 3160 (1991).
  - [6] I. Affleck, A. W. W. Ludwig, H.-B. Pang, and D. L. Cox, Phys. Rev. B **45**, 7918 (1992).
  - [7] I. Affleck and A. W. Ludwig, Physical Review B **48**, 7297 (1993).
  - [8] O. Parcollet and A. Georges, Phys. Rev. Lett. **79**, 4665 (1997).
  - [9] I. Affleck, Journal of the Physical Society of Japan **74**, 59 (2005).
  - [10] V. J. Emery and S. Kivelson, Phys. Rev. B **46**, 10812 (1992).
  - [11] D. G. Clarke, T. Giamarchi, and B. I. Shraiman, Phys. Rev. B **48**, 7070 (1993).
  - [12] G. Zaránd and J. von Delft, Phys. Rev. B **61**, 6918 (2000).
  - [13] J. von Delft, G. Zaránd, and M. Fabrizio, Phys. Rev. Lett. **81**, 196 (1998).
  - [14] A. J. Schofield, Phys. Rev. B **55**, 5627 (1997).
  - [15] R. Bulla, T. A. Costi, and T. Pruschke, Rev. Mod. Phys. **80**, 395 (2008).
  - [16] H. B. Pang and D. L. Cox, Phys. Rev. B **44**, 9454 (1991).
  - [17] N. Andrei and C. Destri, Phys. Rev. Lett. **52**, 364 (1984).
  - [18] A. M. Tsvelick and P. B. Wiegmann, Zeitschrift für Physik B Condensed Matter **54**, 201 (1984).
  - [19] A. M. Tsvelick, Journal of Physics C: Solid State Physics **18**, 159 (1985).
  - [20] N. Andrei and A. Jerez, Phys. Rev. Lett. **74**, 4507 (1995).
  - [21] G. Zaránd, T. Costi, A. Jerez, and N. Andrei, Phys. Rev. B **65**, 134416 (2002).
  - [22] A. M. Sengupta and A. Georges, Phys. Rev. B **49**, 10020 (1994).

- [23] M. Fabrizio, A. O. Gogolin, and P. Nozières, Phys. Rev. Lett. **74**, 4503 (1995).
- [24] P. Coleman, L. B. Ioffe, and A. M. Tsvelik, Phys. Rev. B **52**, 6611 (1995).
- [25] M. Fabrizio, A. O. Gogolin, and P. Nozières, Phys. Rev. B **51**, 16088 (1995).
- [26] S. Pal, A. Mukherjee, and S. Lal, New J. Phys. **21**, 023019 (2019).
- [27] A. Mukherjee, S. Patra, and S. Lal, Journal of High Energy Physics **04**, 148 (2021).
- [28] S. Patra and S. Lal, Phys. Rev. B **104**, 144514 (2021).
- [29] A. Mukherjee and S. Lal, J. Phys.: Condens. Matter **34**, 275601 (2022).
- [30] A. Mukherjee, A. Mukherjee, N. S. Vidhyadhiraja, A. Taraphder, and S. Lal, Phys. Rev. B **105**, 085119 (2022).
- [31] P. W. Anderson, Journal of Physics C: Solid State Physics **3**, 2436 (1970).
- [32] A. Mukherjee and S. Lal, Nuclear Physics B **960**, 115170 (2020).